

# Carbon 13 NMR Studies of Saturated Fatty Acids Bound to Bovine Serum Albumin

## I. THE FILLING OF INDIVIDUAL FATTY ACID BINDING SITES\*

(Received for publication, September 10, 1986)

David P. Cistola, Donald M. Small, and James A. Hamilton

From the Biophysics Institute, Housman Medical Research Center, Departments of Medicine and Biochemistry, Boston University School of Medicine, Boston, Massachusetts 02118-2394

<sup>13</sup>C NMR chemical shift and intensity results for a series of carboxyl <sup>13</sup>C-enriched saturated fatty acids (8–18 carbons) bound to bovine serum albumin (BSA) are presented as a function of increasing fatty acid (FA)/BSA mole ratio. Spectra for long-chain (≥12 carbons) FA·BSA complexes exhibited up to five FA carboxyl resonances, designated *a*, *b*, *b'*, *c*, and *d*. Only three resonances (peaks *b*, *b'*, and *d*) were observed below 3:1 FA·BSA mole ratio, and at ≥3:1 mole ratio, two additional resonances were observed (peaks *c* and *a*). In a spectrum of 5:1 stearic acid·BSA complexes, peaks *b*, *b'*, and *d* each represented approximately one-fifth, and peak *c* approximately two-fifths, of the total FA carboxyl intensity. Plots of total carboxyl/carbonyl intensity ratio as a function of FA·BSA mole ratio were linear up to 7–9 mole ratio. Deviation from linearity at mole ratios ≥7 was accompanied by the detection of crystalline unbound FA (as 1:1 acid/soap) by x-ray diffraction. In contrast to long-chain FA·BSA complexes, <sup>13</sup>C NMR spectra of octanoic acid·BSA complexes yielded only one FA carboxyl resonance (peak *c*) at FA·BSA mole ratios between 1 and 20. We conclude: (i) peaks *b*, *b'*, and *d* represent FA bound to three individual high affinity (primary) long-chain FA binding sites on BSA; (ii) peak *c* represents FA bound to several secondary long-chain (or primary short-chain) FA binding sites on BSA; (iii) peak *a* represents long-chain FA bound to an additional lower affinity binding site. We present a model that correlates the observed <sup>13</sup>C NMR resonances with individual binding site locations predicted by a recent three-dimensional model of BSA.

Utilization of circulating FFA<sup>1</sup> by tissues is influenced not only by the avidity of FFA for and the blood flow through

\* This research was supported by United States Public Health Service Grants HL-26335 and HL-07291. This work was originally submitted in partial fulfillment of the degree of Doctor of Philosophy at Boston University (Cistola, 1985), and preliminary accounts of portions of this work have been published in abstract form (Cistola *et al.*, 1983). The costs of publication of this article were defrayed in part by the payment of page charges. This article must therefore be hereby marked "advertisement" in accordance with 18 U.S.C. Section 1734 solely to indicate this fact.

<sup>1</sup> The abbreviations used are: FFA, free (nonesterified) fatty acid(s); FA, fatty acid(s); BSA, bovine serum albumin; NOE, nuclear Overhauser enhancement; C<sub>8,0</sub>, octanoic acid; C<sub>12,0</sub>, dodecanoic (lauric) acid; C<sub>14,0</sub>, tetradecanoic (myristic) acid; C<sub>16,0</sub>, hexadecanoic (palmitic) acid; C<sub>18,0</sub>, octadecanoic (stearic) acid; C<sub>18,1</sub>, oleic acid. The use of the abbreviation "FA" or the numerical abbreviations for individual FA compounds is not meant to imply anything about the ionization state of the FA carboxyl group.

each tissue, but also by the mole ratio of FFA to albumin in the circulation (Scow and Chernick, 1970; Spector and Fletcher, 1978). In normal human subjects, this ratio is variable and is elevated under certain metabolic or environmental conditions such as fasting (Frederickson and Gordon, 1958) and/or prolonged exercise (Havel *et al.*, 1967). Under certain pathological conditions, FFA/albumin ratios may be transiently or consistently elevated secondary to increased FFA mobilization (diabetic ketoacidosis, myocardial infarction, acute anxiety) or decreased circulating albumin (nephrotic syndrome, liver disease, familial hypoalbuminemia). It is conceivable that increased FFA production and/or decreased circulating albumin could result in abnormal partitioning of FFA into other components of the circulation (lipoproteins, blood cell membranes, endothelial cell membranes; Spector and Fletcher, 1978). This abnormal FFA partitioning might result in detrimental structural and/or functional alterations such as decreased neutrophil phagocytic and bacteriocidal activity (Hawley and Gordon, 1976), platelet aggregation (Hoak *et al.*, 1970), and endothelial cell damage (Zilvermit, 1976).

As one approach to predicting FFA/albumin interactions at different mole ratios *in vivo*, the FA binding properties of albumin have been extensively examined *in vitro* using several approaches (for a review, see Spector, 1975). Binding data obtained from equilibrium partitioning methods have been analyzed by the Scatchard model (Scatchard, 1949) or the stepwise association model (Klotz *et al.*, 1946; Spector *et al.*, 1971). The Scatchard analyses for long-chain FA bound to human (Goodman, 1958) and bovine (Spector *et al.*, 1969) albumin have yielded the concept of three classes of FA binding sites with respect to relative affinities. In contrast, the stepwise association analyses assumed no grouping of binding constants into classes and suggested that this grouping is somewhat arbitrary (Spector *et al.*, 1971; Ashbrook *et al.*, 1975). Second, mapping studies using peptide fragments (King and Spencer, 1970; King, 1973; Reed *et al.*, 1975), chemical modifications (Koh and Means, 1979), or affinity labeling (Lee and McMenemy, 1980) have aided in the localization of ligand binding sites to general regions on the polypeptide sequence. However, pitfalls include possible disruptive changes in protein conformation and binding properties following fragmentation, inconsistencies in affinity labeling, and a lack of specificity with chemical modification (Brown and Schockley, 1982). Third, spectroscopic studies using fluorescence (Sklar *et al.*, 1977; Berde *et al.*, 1979), ESR (Kuznetsor *et al.*, 1975; Morrisett *et al.*, 1975; Rehfield *et al.*, 1978; Perkins *et al.*, 1982), and NMR (Müller and Mead, 1973; Inoue *et al.*, 1979) spectroscopy have yielded information concerning the physicochemical interactions of ligands and

albumin. However, pitfalls include the need for fatty acids containing structure-perturbing spin-label probes (ESR) or conjugated double bonds (fluorescence). Also, <sup>13</sup>C NMR at natural abundance has been hampered by a lack of sensitivity (Kragh-Hansen and Riisom, 1976).

As an alternative approach, we have utilized <sup>13</sup>C NMR spectroscopy with <sup>13</sup>C-enriched fatty acids to investigate the interactions of biologically important FA with bovine albumin. Carbon 13 enrichment greatly enhances spectral sensitivity and permits investigation of FA/albumin interactions in the range of physiologically relevant FA/albumin mole ratios. Using this approach, we have shown that the carboxyl chemical shift of oleic acid bound to BSA is highly sensitive to the FA binding environment on albumin; spectra revealed multiple FA carboxyl resonances corresponding to multiple FA binding environments (Parks *et al.*, 1983). In addition, we have utilized fatty acids with <sup>13</sup>C enrichment in hydrocarbon chain carbons (C-3, C-14) to probe the interactions of myristic acid with BSA (Hamilton *et al.*, 1984).

This paper presents <sup>13</sup>C NMR results for a series of carboxyl <sup>13</sup>C-enriched saturated fatty acids (8–18 carbons) bound to BSA as a function of increasing FA·BSA mole ratio. The results provide direct physicochemical information regarding the order of filling and saturation of individual FA binding sites with increasing FA·BSA ratio as well as the relative occupation of individual sites at a given mole ratio. Second, the results delineate differences between shorter chain and longer chain FA with regard to the number and type of FA binding sites. Third, accompanying powder x-ray diffraction results provide information about the physical state of unbound FA at high mole ratios. Finally, the results permit direct correlation of observed NMR resonances with the FA binding sites predicted by recent models of BSA structure (Brown and Shockley, 1982) and provide insights into the binding locations of FA at different FA/albumin ratios *in vivo*.

#### EXPERIMENTAL PROCEDURES

**Materials**—Essentially FA-free crystallized lyophilized BSA was purchased from Sigma (A-7511, lot 22F-9340). The supplier used method IV of Cohn *et al.* (1947) to recrystallize fraction V albumin and the charcoal defatting procedure of Chen (1967) to remove bound fatty acid. The content of bound fatty acid, as determined by gas-liquid chromatography, was <0.02 mol of FA/mol of BSA prior to the addition of FA. The protein content of the BSA sample was analyzed by sodium dodecyl sulfate-polyacrylamide gel electrophoresis; the gels were overloaded with sample in order to search for minor impurities. In addition to the major albumin band at 66,000 daltons, minor bands were observed at ~120,000 (~5%), 55,000 (<1%), and 160,000 (<1%). These minor bands most likely corresponded to BSA dimers (Friedl and Kistler, 1970; Foster, 1977), α<sub>1</sub>-antitrypsin (Laurell and Jeppsson, 1975), and immunoglobulins, respectively (Putnam, 1975; Peters, 1975). Although apoprotein A-I is often present as a contaminant in commercial albumin preparations (Fainaru and Deckelbaum, 1979), no bands were observed at the appropriate molecular weight (28,000).

The dimer/polymer content of Sigma A-7511 BSA (with added FA), as determined by column chromatography (Parks *et al.*, 1983), was 25%. To determine whether NMR results were affected by the presence of disulfide-linked dimers and polymers, Sigma BSA was further fractionated by gel filtration chromatography. A 2-ml aliquot of hydrated BSA (100 mg/ml) was applied to a column of Sephadex G-150 (90 × 2.6 cm) equilibrated with 20 mM KCl, 0.1% NaN<sub>3</sub> at 4 °C. Fractions of 6 ml were collected at a flow rate of 7 ml/h. The protein concentration of each fraction was determined by its absorbance at 279 nm. The elution profile was essentially identical to one previously published (Morrisett *et al.*, 1975). Fractions containing monomeric BSA were pooled and concentrated by ultrafiltration using Amicon (Danvers, MA) PM-10 filters. The final monomeric BSA sample contained 1.8 ml of 60 mg/ml BSA. No reformation of dimers/oligomers occurred in the concentrated monomeric fraction, as determined by sodium dodecyl sulfate-polyacrylamide gel electro-

phoresis. <sup>13</sup>C NMR spectra for C<sub>14:0</sub>·BSA complexes using monomeric or unfractionated BSA (obtained under identical conditions) were indistinguishable. This result is consistent with our previous observations for C<sub>18:1</sub>·BSA complexes (Parks *et al.*, 1983).<sup>2</sup> Therefore, unfractionated BSA was used throughout this study.

<sup>13</sup>C carboxyl-enriched (90%) fatty acids were purchased from KOR Isotopes (Cambridge, MA) (C<sub>8:0</sub>, C<sub>12:0</sub>, C<sub>16:0</sub>, C<sub>18:0</sub>) and Merck Sharp and Dohme Isotopes (St. Louis, MO) (C<sub>14:0</sub>). Sample purity as determined from thin layer chromatography (hexane:diethyl ether:acetic acid, 90:9:1) was >98%. In addition, no impurities were visualized by <sup>1</sup>H NMR for <sup>13</sup>C-enriched FA samples dissolved in deuterated chloroform.

**Sample Preparation**—BSA solutions (7%, w/v) were prepared using doubly distilled deionized water. After adjusting the pH to 7.4, the solutions were centrifuged at 10,000 rpm for 30 min to remove trace amounts of particulate matter. The protein concentration was determined from the absorbance at 279 nm of 1:100 dilutions using an extinction coefficient of 6.67 for a 1% sample (Janatova *et al.*, 1968). Crystals of <sup>13</sup>C-enriched FA were dissolved in 2:1 chloroform/methanol, and the concentrations were determined by measuring dry weights on an electrobalance (Cahn model 25, Cerritos, CA). Stoichiometric amounts of fatty acids in solvent were added to 10-mm NMR tubes, and the solvent was evaporated under N<sub>2</sub>. D<sub>2</sub>O (200 μl) and 1.2 eq of 1 N KOH were added, and samples were thoroughly mixed until all FA crystals dissolved to form an optically clear micellar soap solution. Hydrated BSA samples (1.8 ml, pH 7.4) were added to the soap solutions (0.2 ml) with continuous vortexing for several minutes, and samples were equilibrated and intermittently vortexed for 30 min. Potassium stearate solutions formed a gel phase at room temperature and had to be gently and briefly heated before BSA solutions were added. Sample pH was adjusted from pH 7.5–7.6 (following mixing) to 7.4 and samples were equilibrated at room temperature (25 °C) for 8–12 h prior to <sup>13</sup>C NMR experiments. The NMR results were independent of equilibration time.

All pH measurements were made directly in the NMR tube using a pH meter (Beckman 3560, Fullerton, CA) equipped with a 29 cm × 4 mm glass combination electrode (Markson MiraMark, Phoenix, AZ). Values measured before and after obtaining NMR spectra agreed within 0.1 pH unit.

The final FA·BSA samples used for NMR contained from 0.5 to 20 mol of FA/mol of BSA and 7% w/v protein. As reported elsewhere (Cistola, 1985), <sup>13</sup>C NMR spectra (FA as well as protein resonances) for C<sub>16:0</sub>·BSA complexes at 3.8, 7.5, and 11.4% w/v BSA (all at 5:1 mol ratio, pH 7.4, 35 °C) were essentially identical. Hence, it is unlikely that noncovalent protein aggregation occurred over this concentration range. The salt concentrations (as determined by flame photometry) of 7% hydrated samples with no added salt were 7 mM (sodium) and 6 mM (potassium). No salt was added to FA·BSA samples in this study. Addition of KCl to FA·BSA samples up to a final concentration of 0.1 M does not change <sup>13</sup>C NMR results provided that the sample temperature is kept below 38 °C (Cistola, 1985).

**Carbon 13 NMR Spectroscopy**—<sup>13</sup>C NMR spectra were obtained on a Bruker WP-200 NMR spectrometer at 50.3 MHz as described elsewhere (Hamilton and Small, 1981; Cistola *et al.*, 1982). Internal D<sub>2</sub>O was used as a lock and shim signal. Chemical shift values were measured digitally with an estimated uncertainty of ±0.1 ppm. The chemical shift (δ = 39.57 ppm) of the narrow resonance from protein ε-Lys/β-Leu carbons (Gurd and Keim, 1973) was used as an internal reference after calibrating this resonance against external tetramethylsilane. To enhance spectral resolution in selected cases, the convolution difference method was used (Campbell *et al.*, 1973). FA carboxyl/BSA carbonyl intensity ratios were measured using the integration routine provided in the Bruker DISNMR program. NMR sample temperatures were controlled to 34 °C and measured as described previously (Cistola *et al.*, 1982). Spin-lattice relaxation times (T<sub>1</sub>) were measured using a fast inversion recovery technique (Canet *et al.*, 1975) and calculated using a three-parameter fitting routine (Sass and Ziessow, 1977). Nuclear Overhauser enhancements (NOE) were determined from comparisons of peak heights from spectra accumulated with broad-band and inverse-gated decoupling (Opella *et al.*, 1976). For all spectral accumulations, pulse intervals were equal to the T<sub>1</sub> value of the largest FA carboxyl peak in the spectrum, and 90 °C pulses (15 μs) were used.

<sup>2</sup> Note that in our previous study, a 90 × 2.5-cm column was used for preparative fractionation of monomeric BSA, rather than a 90 × 1.5-cm column (incorrectly noted in Fig. 1 caption of Parks *et al.*, 1983).

**X-ray Diffraction**—For samples containing suspended crystalline material (>7:1 FA·BSA), the material was pelleted by centrifugation at 10,000 rpm for 30 min at 30 °C. The pellet was transferred to 1-mm quartz capillary tubes (Charles Supper Co., Natick, MA), and the capillaries were placed in a sample holder kept at constant temperature (30 °C) by a circulating antifreeze/water bath. Nickel-filtered  $\text{CuK}\alpha$  x-radiation ( $\lambda = 1.5418 \text{ \AA}$ ) from a microfocus x-ray generator (Jarrell-Ash, Waltham, MA) was focused by a single nickel-coated mirror and further collimated by a Luzzati-Baro camera with slit optics. Low-angle powder x-ray diffraction patterns were recorded with a position-sensitive detector (Tennelec PSD-1100, Oak Ridge, TN) and a computer-based analysis system (Tracor Northern TN-1710, Middleton, WI).

## RESULTS

$^{13}\text{C}$  NMR spectra at various  $\text{C}_{14:0}$ -BSA mole ratios (at fixed pH, BSA concentration, ionic strength, and temperature) are shown in Fig. 1, A–E. The broad envelope centered at ~176 ppm represents carbonyl carbons of glutamine, asparagine, and the peptide backbone (Gurd and Keim, 1973) as well as aspartate carboxyl carbons (Shindo and Cohen, 1976) of BSA. The narrower resonances falling between 179 and 184 ppm primarily represent carboxyl carbons of  $^{13}\text{C}$ -carboxyl-enriched FA bound to BSA (Parks *et al.*, 1983; Cistola *et al.*, 1983; Hamilton *et al.*, 1984), except for the resonance at 180.9–181.1 ppm, which represents protein glutamate carboxyl carbons (Shinodo and Cohen, 1976). Protein-free saturated FA (>10 carbons) exist as crystalline 1:1 acid/soap compounds at pH 7.4 and 35 °C (Cistola *et al.*, 1986), and crystalline phases do not give rise to high resolution NMR resonances. Furthermore, none of the observed carboxyl resonances had chemical shifts coincident with those of soluble short-chain FA in water (without protein) under the same conditions (Cistola *et al.*, 1982; Cistola, 1985). Hence, the observed carboxyl resonances do not represent unbound FA. In addition, none of these resonances represented BSA peaks that shifted into the carboxyl region upon FA binding, since spectra of FA·BSA complexes using  $\text{C}_{14:0}$  with no  $^{13}\text{C}$  enrichment were identical to FA-free BSA samples (Fig. 1A). In order to compare FA carboxyl peaks in different FA·BSA spectra, we have named analogous FA carboxyl peaks, based on their chemical shifts at pH 7.4 (and their ionization behavior; Cistola *et al.*, 1987), as follows: peak *a* (183.7–184.1 ppm), peak *b* (182.5 ppm), peak *b'* (182.2–182.4 ppm), peak *c* (181.8–182.1 ppm), and peak *d* (180.4–180.7 ppm). In addition, we have named the glutamate carboxyl resonance as peak *pr* (180.9–181.1 ppm). It is notable that peak *b'* was not observed for  $\text{C}_{18:1}$ -BSA complexes (Parks *et al.*, 1983) either because peak *b'* was not present or because it was not resolved from peaks *b* and *c*.

For most of the FA·BSA spectra presented in this study, the intensities of *individual* FA carboxyl peaks could not be quantitatively measured as peak areas or peak heights because of closely overlapping FA or protein carboxyl resonances. Therefore, increases in FA carboxyl peak intensity with increasing mole ratio are represented qualitatively in the form of difference spectra. Digital subtraction of the upper spectra from the lower spectra yielded the difference spectra shown in the right column of Fig. 1 (F–I). The difference spectra contained only those FA carboxyl peaks which increased or decreased in intensity or changed chemical shifts between the two different mole ratios. The intensities resulting from unperturbed carboxyl or carbonyl resonances of BSA were subtracted out by this procedure.

At 1:1 mole ratio (Fig. 1B), peaks *b* and *b'* were clearly visible, but peak *d* was difficult to distinguish because of closely overlapping protein glutamate resonance(s). However, subtraction of FA-free BSA (Fig. 1A) from 1:1  $\text{C}_{14:0}$ -BSA (Fig. 1B) revealed that peak *d* was present at 1:1 mole ratio (Fig.

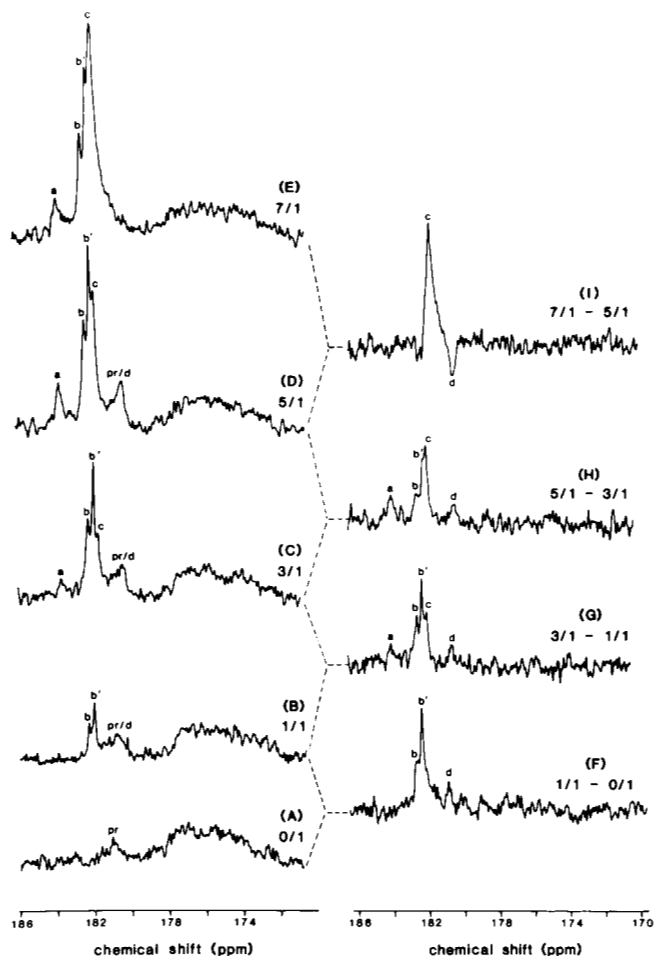


**FIG. 1. Carboxyl/carbonyl region of  $^{13}\text{C}$  NMR spectra (A–E) and difference spectra (F–I) for  $\text{C}_{14:0}$ -BSA complexes with different  $\text{C}_{14:0}$ -BSA mole ratios at pH 7.4 and 34 °C.** Difference spectra were obtained by digitally subtracting a spectrum at a given mole ratio from one at a higher mole ratio. This method removes BSA resonances from spectra and shows which FA carboxyl resonances increased between two corresponding FA·BSA mole ratios. The pairs of spectra which were subtracted are indicated by the dashed lines in the middle of the figure. The lower case letters above each peak indicate specific FA carboxyl resonances with characteristic chemical shifts (see “Results”). For all samples, the BSA concentration was 7% (w/v). All spectra were recorded after 6,000 accumulations with a pulse interval of 2.0 s, 16,384 time domain points, and a spectral width of 10,000 Hz. Line broadening (3 Hz) was used in all spectral processing. A, FA-free BSA spectrum; B, 1:1  $\text{C}_{14:0}$ -BSA spectrum; C, 3:1  $\text{C}_{14:0}$ -BSA spectrum; D, 5:1  $\text{C}_{14:0}$ -BSA spectrum; E, 7:1  $\text{C}_{14:0}$ -BSA spectrum; F, difference spectrum, 1:1  $\text{C}_{14:0}$ -BSA minus FA-free BSA; G, difference spectrum, 3:1  $\text{C}_{14:0}$ -BSA minus 1:1  $\text{C}_{14:0}$ -BSA; H, difference spectrum, 5:1  $\text{C}_{14:0}$ -BSA minus 3:1  $\text{C}_{14:0}$ -BSA; I, difference spectrum, 7:1  $\text{C}_{14:0}$ -BSA minus 5:1  $\text{C}_{14:0}$ -BSA.

1F). Between 1:1 and 3:1 mole ratio (Fig. 1, B, C, and G), peaks *b*, *b'*, and *d* increased, and peaks *c* and *a* appeared above 2:1 mole ratio (2:1 spectrum not shown). Between 3:1 and 5:1 mole ratio (Fig. 1, C, D, and H), intensity increases occurred in all five FA carboxyl peaks. Between 5:1 and 7:1 mole ratio (and up to 13:1 mole ratio), only peak *c* increased in intensity (Fig. 1, D, E, and I). Peak *d* decreased in intensity between 5:1 and 7:1 mole ratio (Fig. 1I).

A plot of *total* carboxyl/carbonyl area ratio as a function of  $\text{C}_{14:0}$ -BSA mole ratio is shown in Fig. 2 (circles). The plot is linear up to 8–9:1 mole ratio, above which point the sample became increasingly turbid (suspended crystals; downward pointing arrow in Fig. 2). The samples were centrifuged and yielded a transparent supernatant and a crystalline pellet.

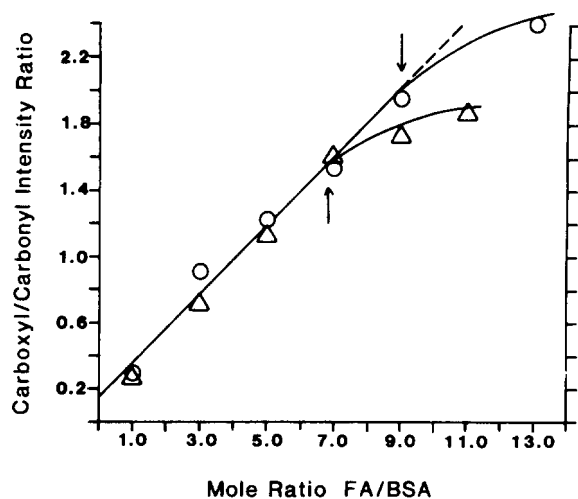


FIG. 2. Plots of total  $^{13}\text{C}$  NMR carboxyl intensity relative to total carbonyl intensity as a function of FA:BSA mole ratio for  $\text{C}_{14.0}$ -BSA (○—○) and  $\text{C}_{16.0}$ -BSA (△—△). The arrows indicate the mole ratio at and above which turbidity and crystalline precipitate were visualized in  $\text{C}_{14.0}$ -BSA (arrow pointing downward) and  $\text{C}_{16.0}$ -BSA (arrow pointing upward) samples. The dashed line indicates the expected (extrapolated) intensity ratio if essentially all FA were protein associated. FA not associated with protein under these conditions was crystalline and would not contribute to the total NMR carboxyl intensity. Note that the absolute values of the intensity ratios are arbitrary and have no direct stoichiometric meaning.

Examination of the pellet by powder x-ray diffraction showed first order long spacings ( $41.0 \pm 0.9\text{Å}$ ) characteristic for crystalline 1:1 potassium (or sodium) hydrogen dimyristate, a 1:1 acid/soap compound (Piper, 1929; Cistola *et al.*, 1986). Therefore  $\text{C}_{14.0}$ -BSA samples at high mole ratio contained unbound FA in the form of crystalline 1:1 acid/soap. In general, long-chain fatty acids in water ( $\geq$ micromolar concentrations) form 1:1 acid/soap crystals or fatty acid/soap lamellar liquid crystals between pH 7 and 10 (Small, 1986).<sup>3</sup>

$^{13}\text{C}$  NMR spectra and difference spectra at various  $\text{C}_{18.0}$ -BSA mole ratios are shown in Fig. 3, A–I. At 1:1 mole ratio, peaks *b*, *b'*, and *d* were present (Fig. 3, B and F), although peak *d* was barely detectable. Peak *d* was much more clearly seen at 2:1 (spectrum not shown) and 3:1 (Fig. 3, C and G). Between 1:1 and 3:1 mole ratio, peaks *b*, *b'*, and *d* increased in intensity (Fig. 3, B, C, and G). Between 3:1 and 5:1 mole ratio, peaks *c* and *a* became visible and all five FA carboxyl peaks increased in intensity (Fig. 3, C, D, and H), and between 5:1 and 7:1 (spectrum not shown), peaks *c*, *b/b'*, and *a* increased in intensity (Fig. 3, D, E, and I).

A plot of total carboxyl/carbonyl area ratio as a function of  $\text{C}_{18.0}$ -BSA mole ratio (not shown) was linear up to about 7:1 mole ratio. Deviation from linearity was accompanied by the visual appearance of sample turbidity (suspended crystals) at and above 7:1 mole ratio. As with  $\text{C}_{14.0}$ /BSA (see above), these crystals most likely represent unbound  $\text{C}_{18.0}$  in the form of crystalline 1:1 acid/soap.

$^{13}\text{C}$  NMR spectra (but not difference spectra) for  $\text{C}_{12.0}$ -BSA complexes at four mole ratios are shown in Fig. 4. These spectra were very similar to corresponding spectra for  $\text{C}_{14.0}$ -BSA complexes. At 1:1 mole ratio, peaks *b/b'* and *pr/d* were visualized; at 3:1, three FA peaks were visualized (*b*, *b'*, *d*). At 5:1 and 7:1 mole ratios, all five FA carboxyl peaks were distinguishable. Convolution difference spectra (not shown) permitted greater resolution of peaks *b* and *b'*.

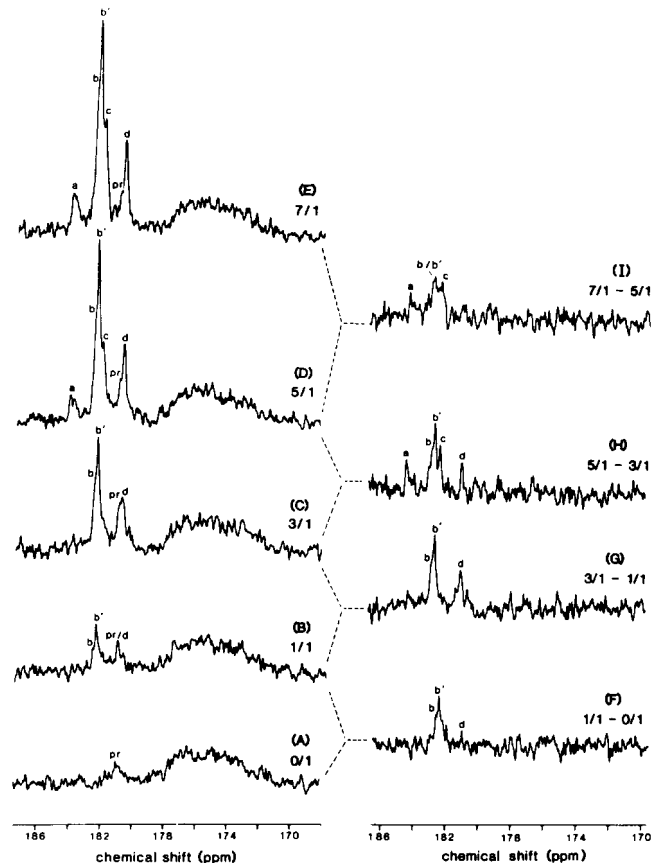


FIG. 3. Carboxyl/carbonyl region of  $^{13}\text{C}$  NMR spectra (A–E) and difference spectra (F–I) for  $\text{C}_{18.0}$ -BSA complexes with increasing  $\text{C}_{18.0}$ -BSA mole ratio at pH 7.4, 34 °C. The lower case letters above each peak indicate specific FA carboxyl resonances with characteristic chemical shifts (see “Results”). Spectra were recorded after 6000 accumulations with a pulse interval of 2.7 s. All other spectral conditions and explanations are as described in the legend to Fig. 1.

A plot of total carboxyl/carbonyl area ratio as a function of  $\text{C}_{12.0}$ -BSA mole ratio (not shown) was essentially identical to that for  $\text{C}_{14.0}$ -BSA (Fig. 2, circles). Deviation from linearity and the appearance of sample turbidity (crystal formation) occurred above 8–9:1 mole ratio. Centrifugation and examination of crystals by powder x-ray diffraction revealed first order long spacings ( $35.4 \pm 0.7\text{Å}$ ) characteristic for crystalline 1:1 potassium (or sodium) hydrogen laurate, an acid/soap compound (Cistola *et al.*, 1986).

$^{13}\text{C}$  NMR spectra for  $\text{C}_{16.0}$ -BSA complexes as a function of mole ratio (Cistola, 1985) are not shown here and were essentially identical to those for  $\text{C}_{18.1}$ -BSA complexes (Parks *et al.*, 1983). A plot of total carboxyl/carbonyl area ratio as a function of  $\text{C}_{16.0}$ -BSA mole ratio is shown in Fig. 2 (triangles). Deviation from linearity and sample turbidity (crystals) appeared at and above 7:1 mole ratio. The crystals most likely represented crystalline 1:1 acid/soap, as was demonstrated by x-ray diffraction, for  $\text{C}_{12.0}$ -BSA and  $\text{C}_{14.0}$ -BSA samples.

Although peaks *b*, *b'*, and *c* closely overlapped in many FA-BSA spectra, peaks *d* and *a* were nearly completely resolved from the *b/b'/c* envelope, and their relative intensities (areas) could be quantitatively estimated (Table I). To determine the relative area of peak *d*, the area from the glutamate carboxyl resonance (peak *pr*) had to be subtracted out (see legend to Table I). The results indicate that the relative intensities of peak *d* increased and peak *a* decreased, with increasing FA chain length. However, the relative intensity of the *b/b'/c*

<sup>3</sup> D. P. Cistola, J. A. Hamilton, D. Jackson, and D. M. Small (1987) *Biochemistry*, submitted for publication.

TABLE I  
Relative <sup>13</sup>C NMR intensities of peaks a and d

The areas of all resonances were measured by integration (see "Experimental Procedures"). The areas of peak d and the total FA carboxyl region were determined by subtracting out the contribution of BSA glutamate carboxyl resonances. This glutamate contribution (glutamate/carbonyl ratio) was determined from spectra of FA-free BSA accumulated under the same conditions as FA/BSA spectra. All three samples reported in this table contained 5:1 mole ratio of FA/BSA. C<sub>14,0</sub>-BSA and C<sub>18,0</sub>-BSA results were derived from spectra shown in Figs. 1D and 3D, respectively, and C<sub>16,0</sub>-BSA results were derived from a spectrum not shown here (Cistola, 1985). The estimated uncertainty is ±10%.

	d/a ratio	Total FA carboxyl intensity		
		d	a	b + b' + c
%				
C <sub>14,0</sub> -BSA	0.09	2	20	78
C <sub>16,0</sub> -BSA	0.7	12	19	69
C <sub>18,0</sub> -BSA	2.3	19	8	73

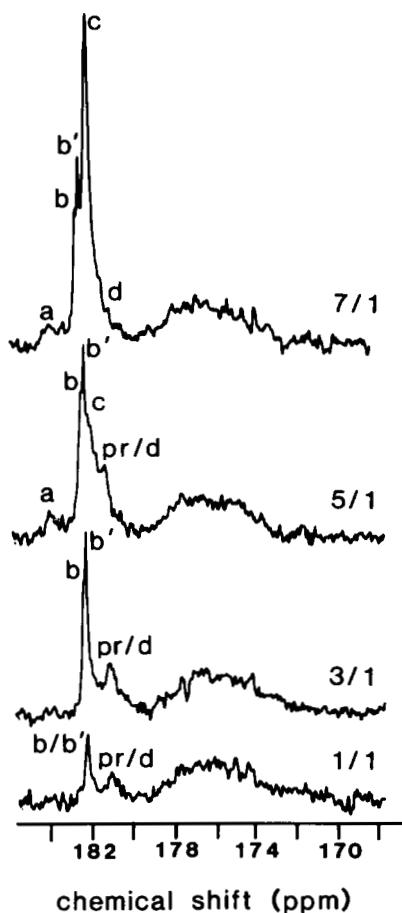


FIG. 4. Carboxyl/carbonyl region of <sup>13</sup>C NMR spectra for 1-<sup>13</sup>C C<sub>12,0</sub>-BSA with increasing C<sub>12,0</sub>-BSA mole ratio at pH 7.4 and 34 °C. The numbers at the right of each spectrum indicate the mole ratio of C<sub>12,0</sub>-BSA. Spectra were recorded after 4000 accumulations with a pulse interval of 2.8 s. All other spectral conditions are as described in the legend to Fig. 1.

envelope exhibited little or no change with increasing FA chain length. (Results for C<sub>12,0</sub>-BSA were not included because peak d was not well resolved from the b-b'-c complex; Fig. 4.)

<sup>13</sup>C NMR spectra for C<sub>8,0</sub>-BSA complexes (Fig. 5), unlike those for all other FA-BSA complexes studied, showed only one FA carboxyl peak at all mole ratios (up to 20:1). At 5:1 mole ratio (pH 7.4), the chemical shift of this resonance was

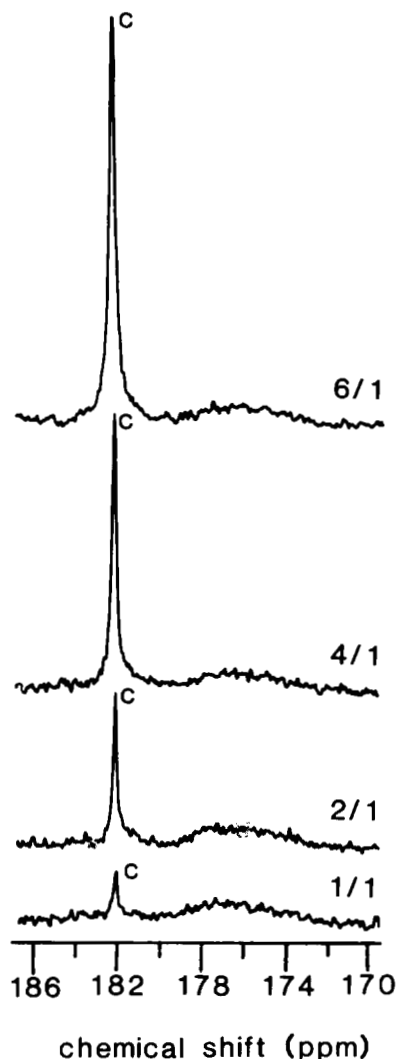


FIG. 5. Carboxyl/carbonyl region of <sup>13</sup>C NMR spectra for 1-<sup>13</sup>C C<sub>8,0</sub>-BSA with increasing C<sub>8,0</sub>-BSA mole ratio at pH 7.4 and 34 °C. The numbers at the right of each spectrum indicate the mole ratio of C<sub>8,0</sub>-BSA. The narrow peaks labeled c are FA carboxyl resonances, and the very broad peaks centered at ~176 ppm correspond to BSA carbonyl resonances. Spectra were recorded after 4000 accumulations with a pulse interval of 2.0 s. All other spectral conditions are as described in the legend to Fig. 1. The BSA concentration was 7.5% (w/v).

182.1 ppm; this value suggested that this FA resonance was analogous to peak c in the other FA-BSA spectra. This correlation was also supported by NMR titration results which demonstrated that peak c was the only one of the five observed FA carboxyl peaks to exhibit a titration shift between pH 7.4 and 3.0 (Cistola *et al.*, 1987). The chemical shift of peak c in C<sub>8,0</sub>-BSA spectra increased with increasing mole ratio from 182.0 ppm (1:1 and 3:1 mole ratio) to 182.1 ppm (5:1), 182.2 ppm (7:1), 182.3 ppm (9:1), and 182.9 ppm (20:1).<sup>4</sup> The line widths of this resonance remained narrow (<10 Hz) at all mole ratios studied.

<sup>4</sup> Unbound C<sub>8,0</sub> under these conditions would have existed as monomers in solution, rather than crystalline or liquid-crystalline aggregates or micelles. For C<sub>8,0</sub> BSA samples at >3:1 mole ratio, a progressive increase in the chemical shift of peak c (see "Results") toward the chemical shift of monomeric aqueous C<sub>8,0</sub> (184.2 ppm) provided evidence that monomeric unbound C<sub>8,0</sub> was present at concentrations >>1 μM and in rapid exchange (>>100 exchanges/s) with protein-bound C<sub>8,0</sub>.

# Explore Litigation Insights

Docket Alarm provides insights to develop a more informed litigation strategy and the peace of mind of knowing you're on top of things.

## Real-Time Litigation Alerts



Keep your litigation team up-to-date with **real-time alerts** and advanced team management tools built for the enterprise, all while greatly reducing PACER spend.

Our comprehensive service means we can handle Federal, State, and Administrative courts across the country.

## Advanced Docket Research



With over 230 million records, Docket Alarm's cloud-native docket research platform finds what other services can't. Coverage includes Federal, State, plus PTAB, TTAB, ITC and NLRB decisions, all in one place.

Identify arguments that have been successful in the past with full text, pinpoint searching. Link to case law cited within any court document via Fastcase.

## Analytics At Your Fingertips



Learn what happened the last time a particular judge, opposing counsel or company faced cases similar to yours.

Advanced out-of-the-box PTAB and TTAB analytics are always at your fingertips.

## API

Docket Alarm offers a powerful API (application programming interface) to developers that want to integrate case filings into their apps.

## LAW FIRMS

Build custom dashboards for your attorneys and clients with live data direct from the court.

Automate many repetitive legal tasks like conflict checks, document management, and marketing.

## FINANCIAL INSTITUTIONS

Litigation and bankruptcy checks for companies and debtors.

## E-DISCOVERY AND LEGAL VENDORS

Sync your system to PACER to automate legal marketing.